Appl. Sci. Converg. Technol. 25(1): 7-14 (2016)
http://dx.doi.org/10.5757/ASCT.2016.25.1.7

Review Paper

Nanoplasmonics: An Enabling Platform for Integrated Photonics and Biosensing

Jihye Lee[a,b] and Jong-Souk Yeo[a,b]*
[a]*School of Integrated Technology, Yonsei University, Incheon 406-840*
[b]*Yonsei Institute of Convergence Technology, Yonsei University, Incheon 406-840*

Received January 25, 2015; revised January 30, 2016; accepted January 30, 2016

Abstract Nanoplasmonics is a developing field that offers attractive optical, electrical, and thermal properties for a wide range of potential applications. Based on the compelling characteristics of this field, researchers have shed light on the possibilities of integrated photonics and biosensing platforms using nanoplasmonic principles. Single and unique nanostructures with plasmons can act as individual transducers that convert desired information into measurable and readable signals. In this review, we will discuss nanoplasmonic sensors, especially those in relation to photodetectors for future optical interconnects, and bioinformation sensing platforms based on nanoplasmonics, thus providing a viable approach by which to create sensors corresponding to target applications. In addition, we also discuss scalable fabrication processes for the creation of unconventional nanoplasmonic devices, which will enable next-generation plasmonic devices for wearable, flexible, and biocompatible systems.

Keywords: Plasmonics, Integrated photonics, Plasmon coupling effect, Biomolecule sensing

I. Introduction

A sensing platform is a device that can transform the desired information into useful and readable signals. These platforms can detect changes in targeted environments by converting the relevant change to a measurable form of energy, namely, a transduction [1]. To realize such sensing platforms, there are several types of transduction mechanisms [2], including the electrical [3,4], mechanical [5, 6], optical [7-9], chemical [10], acoustic [11], and thermal types [12]. Specifically, optical transduction principles based on photonic equipment have been studied extensively due to the development of ultrafast femtosecond and picosecond lasers, especially those used for laser-induced breakdown spectroscopy (LIBS), coherent Raman spectroscopy, and terahertz (THz) spectroscopy [13,14]. Optical waveguiding techniques are used for the excitation of fluorescent dye [15] to detect stained cells or target molecules. Photodetectors for sensing light-emitting reporters are also facilitated by a commercialized photomultiplier tube, an avalanche photodiode, and by charge-coupled devices [16]. These high-level conventional photonic approaches are also integrated into various fields, such as IT, energy, and biosystems, by means of the generation, modulation, manipulation, and detection of the associated radiation.

For areas beyond the classical concept of photonics and its sensing applications, the emerging field of light-matter interaction presents promising key words of a new approach [17-19]. This refers to a type of nanophotonics, specifically nanoplasmonics that has been researched rigorously, focusing on the confinement of electromagnetic radiation in sub-wavelength-scale metallic nanostructures [20]. The interaction between light and a nanostructure leads to movement of a free-electron gas in a size-confined metal nanostructure and creates charges moving at opposite displacements with respect to the lattice ions. The opposite displacements of the charges create the restoring force with oscillation known as the surface plasmon (SP). The oscillation frequency of an electromagnetic wave can be determined by the restoring force and the effective mass of an electron [21]. When the incident wave matches the resonance frequency of the oscillation in a metal, the electric fields around the structure are tremendously enhanced, behaving as an electromagnetic dipole and emitting a photon at the same frequency [22]. The re-emitted photon can be seen around the nanostructure and can be tuned by the change of the refractive index around the nanostructure [23-25]. In more detail, the size, shape and materials of the nanostructure are the key factors to consider when tuning the operating wavelength and determining its compatibility with the proposed application [18]. There are various target applications of nanoplasmonics [21], ranging from practical applications such as those in biodiagnosis [26,27], therapeutics [28,29], and cloaking applications combined with metamaterials [30], to security systems for

*Corresponding author
E-mail: jongsoukyeo@yonsei.ac.kr

the generation of encryption keys and for anti-counterfeiting [31,32], information processing, and computing [33-35].

In this review, we discuss the recent development of nanoplasmonic sensing approaches, specifically ranging from optical interconnects to bioapplications. We also discuss the two major transduction mechanisms based on nanoplasmonics. First, the optical signal can be translated into an electrical signal via a nanoplasmonic effect. This transduction mechanism is not only affected by the radiative damping of the nanoplasmonics, but it also relies on non-radiative damping, which can be explained by the change of the photocurrent. In the second approach, biomolecular information can be transduced to an optical read-out signal in beautiful colors. This colorimetric sensing approach, linked by proteins, DNA and RNA, is a powerful concept for home-built point-of-care diagnostic testing (POCT). The final point is that all sensing prototypes stemming from the beauty of nanotechnology require scalable fabrication methods for mass production and integration with other emerging devices by means of a flexible platform. Therefore, we review the unconventional printing techniques of stencil lithography, transfer printing, and imprinting for nanopatterning.

II. Optical Information Transduced to an Electrical Signal by Nanoplasmonics

With ever increasing amount of information and data processing in electronics communication, there is a need for ultra-fast and low-power links between electronics, such as the chip-to-chip and board-to-board interconnects. Conventional and classical interconnections are composed of electrical interconnects [36,37]. Due to the bandwidth limitations in these interconnects, it is necessary to develop a new approach for interconnection with high bandwidths, high responsivity and for straightforward integration with small-scale electronics [38,39]. The successful form of an interconnect which enables a higher processing speed is an optical interconnect for short-range communication that can be combined with electronics to benefit from both super-wide bandwidth of optics and ultra-compact electronics. An optical interconnection between chips and boards requires various photonic components, one of them being an integrative photodetector to translate light into electrical signals. However, optics classically utilize refractive optics and micro-scaled devices, thus introducing the issue of dimensional compatibility when attempting to merge nano-scaled modern electronic devices and conventional photonic components [40].

Overcoming the issues related to photonic integrated circuits, nanoplasmonics offers a novel approach for integrative photodetectors providing good size compatibility with electronics [41-43]. As the approach can couple light to a sub-wavelength nanostructure by forming a resonant mode in femtoseconds [44], this new concept of plasmonic photodetection also enables a rapid detection.

The plasmonic photodetector essentially relies on photo-excited electrons, also known as hot electrons, which can induce a photocurrent in the nanostructure. There are two pathways for energy relaxation of these excited electrons within a femtosecond or picosecond, as shown in Figure 1 [45,46]. An excited electron confined in a nanostructure creates a strong electric field when the resonant mode occurs. The first method of the relaxation of hot electrons is the re-emitting of photons with the same frequency (Figure 1(a)). The emitted photons can be seen in the form of a color of a frequency identical to that of the resonant mode. This relaxation mode is termed a radiative damping. The other mode is called a non-radiative damping. Non-radiative decay, known as Landau damping, refers to the transition of an electron in the intraband within a conduction band or an interband transition from the d band to the sp band [18]. This transition mode generates the electron-hole pair within a femtosecond and excited phonon vibration within a picosecond, as illustrated in Figure 1(b). The additional hot electrons and phonons, called hot carriers, cause electron-electron scattering and electron-phonon scattering within the nanostructure when the relaxation mode occurs. All of the scattering reduces the conductivity of the metal nanostructure, thus decreasing the

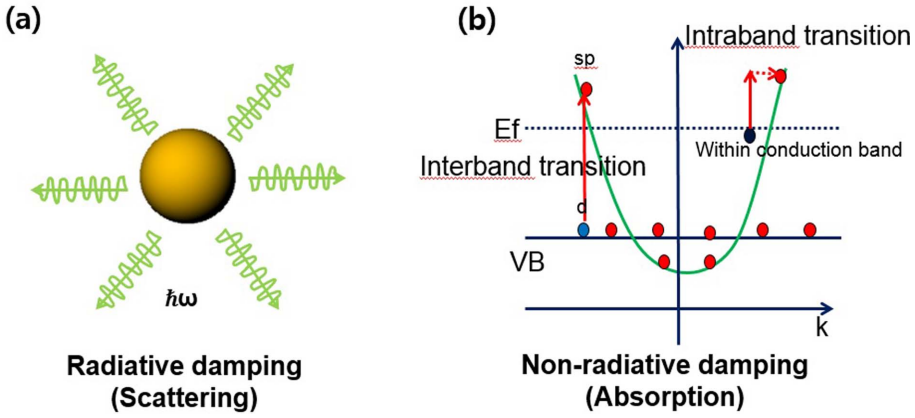

Figure 1. Schematics of (a) radiative damping and (b) non-radiative damping.

photocurrent, known as a negative photocurrent. Shape and structure dependent characteristics of surface plasmons led to the development of various types of plasmonic photodetection. For example, corrugated metal gratings have been combined with a semiconductor structure [47-49]. A nanowire structure was also demonstrated in the form of a metal-semiconductor-metal (MSM) detector for high-speed operation [44,50]. Moreover, single-hole or single-slit-shaped detectors have been developed for good responsivity due to the light collection capabilities of these devices [51]. All of these examples wholly depend on the surface plasmon polariton (SPP) along a metal and semiconductor, thus enabling the creation of electron-hole pairs (EHPs) in semiconductors when the incident light is absorbed while generating a photocurrent in the device scheme [52]. Another example of such a mechanism depends on the internal photoemission (IPE), which occurs in three steps: the generation of hot carriers by the absorption of light, the transportation of the carriers to the Schottky contact (from the metal to the semiconductor), and the emission of the carriers in the semiconductors. These SPP-based photodetectors have been used to construct a photodetector in the subwavelength regime compared to the traditionally larger photonic-based detectors. However, there remain challenges, such as the high losses of metallic waveguides, resulting in a very weak plasmon wave, and the decay of the plasmon wave immediately at the interface of the dielectric medium [18, 19,38]. Therefore, new photodetectors have been developed utilizing the localized surface plasmon resonance (LSPR) within small nanoparticles, and the metal nanowires combined with two-dimensional materials. A recent paper written by Kim et al. demonstrated nanoridge-plasmon-based photodetectors for broadband detection with high photoresponsivity and low power consumption [53].

The unique nanoridge structure can confine the broadband wavelength of light in a tapered shape. Figure 2 (a) illustrates nanoridge arrays (NRAs) with photocurrents measured using a probe station and an incoherent halogen lamp with a low power of 0.2-3.5 mW in a visible range spectrum of 400-700 nm. When light is irradiated onto the nanoridge, the current passing through the wire at low bias voltage is greatly reduced owing to the scattering of hot electrons and phonons in the confined wire. This photocurrent is calculated as follows:

$$I_{Photocurrent} = I_{Off} - I_{On}$$

The scattering is caused by the localized surface plasmon resonance for broadband wavelength of visible light due to the ridge shape of the nanowire. Figure 2(c) shows the broadband detection using a gold nanoridge array as measured by dark-field microscopy. The characteristics of the colors are determined by the focused point of the microscopy ranging from the top (blue scattering) to the bottom (red scattering) of the nanoridge cross-section. As the approach offers broadband photodetection with high photoresponsivity and ultrasmall dimension compatible with integrated electronics, the on-chip nanoplasmonic photodetector provides interesting pathway for integrated photonic interconnection and sensing applications.

Another study was recently carried out by Miao et al. using a two-dimensional material and a nanoplasmonic structure, as shown in Figure 3 [54]. A MoS_2 layer is combined with a surface plasmon-enhanced gold array to overcome the low photoresponsivity of MoS_2 due to its low light absorption (Figure 3(a)) [55,56]. With the help of plasmonics, the light is effectively localized in the gold nanoparticles, thus enhancing the electric field around the structure while also improving the light absorption

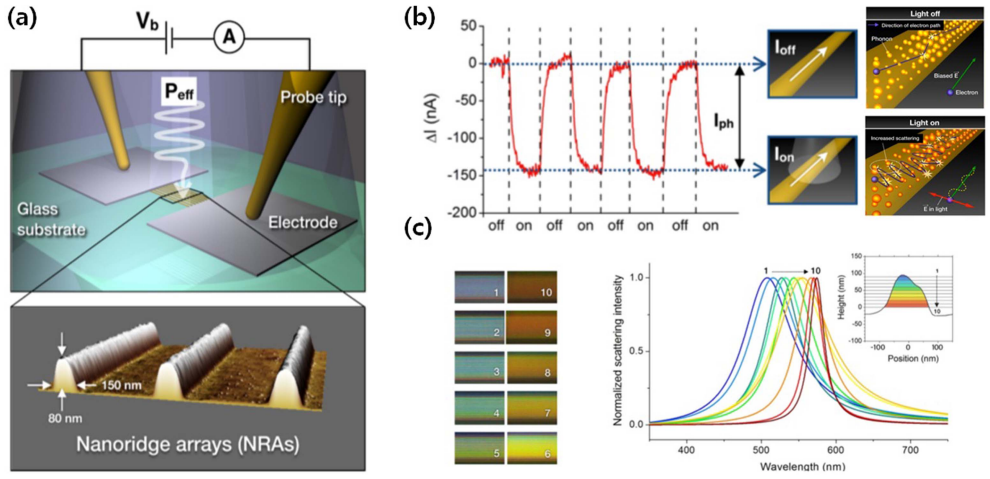

Figure 2. Nanoplasmonic photodetector: (a) Schematic of electrical detection of a photocurrent using nanoridge arrays (NRAs); the bottom figure shows an atomic force microscopy image of the NRAs. (b) Schematic and current response of the NRAs when the light is turned on and off, (c) Optical response of the NRAs showing broadband photodetection as measured by dark-field microscopy and spectrometry (Parts a, b, and c reprinted with permission from 52. Copyright (2015) American Chemical Society).

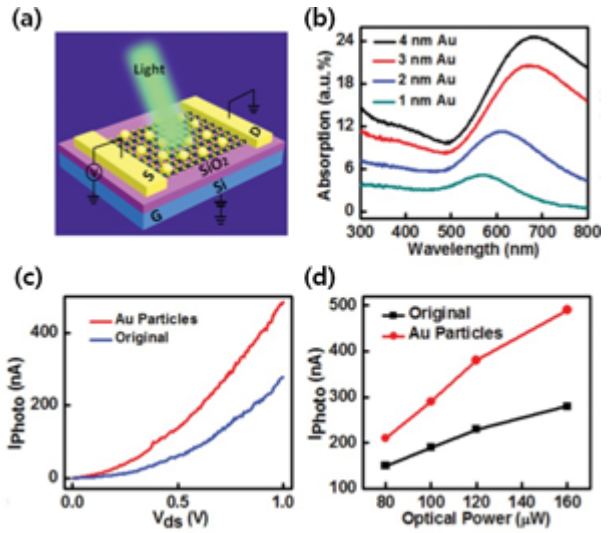

Figure 3. (a) Schematic of few-layer MoS_2 phototransistors: (b) Absorption characteristics of Au nanoparticles on glass as measured by a UV-Vis spectrophotometer. (c) Photocurrent response corresponding to the voltage with or without Au. (d) Photocurrent response corresponding to the illuminated laser power intensity (λ = 632 nm). (Parts a, b, c, and d reprinted with permission from 53 © Wiley).

properties. Figure 3(b) shows the absorption intensity corresponding to the wavelength and thickness of the gold layer. The thickness of the gold layer is important to maximize the absorption of light. Due to the coupling of excited plasmons on the atomically thin MoS_2 layer, an improved photocurrent is generated for the given bias voltage and optical power (Figures 3(c)-(d)). According to the results, merging 2D materials and nanoparticles provides high photoresponsivity and a selectable wavelength in MoS_2 that is also compatible with silicon-based electronics. In addition, it is possible to extend this method with strong plasmon resonance to flexible optoelectronic devices such as image sensors or biosensor arrays.

In conclusion, based on an advanced optical transduction mechanism using nanoplasmonics, highly efficient on-chip photodetection will enable the integration of photonic and electronic systems providing low power, wavelength selectivity, and high responsivity.

III. Bioinformation Transduced into Optical Signal by Nanoplasmonics

There are many research schemes to detect biomolecules for diagnostics and therapeutics. The conventional biosensor, which can transduce biomolecule information into a measurable signal, works via the polymerase chain reaction (PCR) [57] and the enzyme-linked immunosorbent assay (ELISA) [58,59]. These batch-type approaches have high sensitivity and high throughput, but they are expensive to operate, time-consuming and need skillful researchers to prepare them. Another major challenge is the high operating power. These hurdles must be overcome to extend these methods to various applications, such as point-of-care testing (POCT) in developing countries with low resources [60,61]. Nanoplasmonics is a promising means of overcoming the conventional biosensing approach. Single nanoparticles can act as small transducers that convert the biomolecules information into visible signals [62-65]. Fundamental sensing is carried out by radiative damping, as was discussed already. The attachment of biomolecules can change the refractive index of the surrounding nanoparticles, thus dramatically changing the optical responses.

The optical responses with the re-emitting of colors shown as a LSPR spectral peak can be tuned by the type of the biomolecules, its concentration, and the molecular conformation [66]. The shift of the LSPR peak from the particles is approximately described as

$$\Delta\lambda \approx m(n_{absorbate} - n_{medium})(1 - e^{-2d/l}),$$

where m is the sensitivity factor (expressed as nm per refractive index unit (RIU)), $n_{absorbate}$ and n_{medium} are respectively the RIU values of the absorbate molecules and the medium surrounding the environment of the particles, d is the thickness of the absorbed layer and l is the electromagnetic field decay length. The spectral red shift is

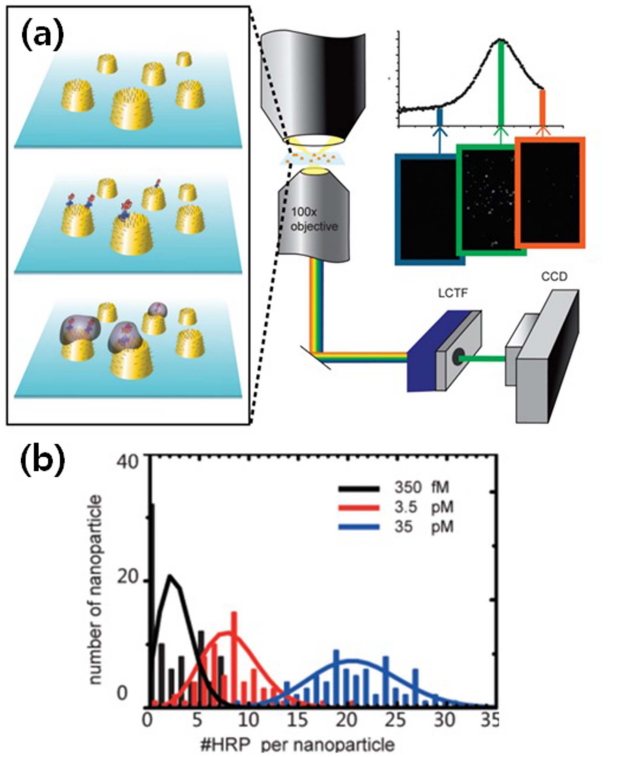

Figure 4. Illustration of (a) gold nanoparticles on glass as functionalized by biotin, and binding of streptavidin and HRP, leading to the precipitation reaction on the surface. The images and discrete wavelengths are shown using dark-field microscopy combined with a tunable narrow-band-pass liquid crystal filter. (b) The calibration curve for the amount of HRP per nanoparticle corresponding to its concentration (Parts a, b, c, and d reprinted with permission from 72, © American Chemical Society).

easily controlled and maximized by considering the proper selection of the nanoparticle shape and size, and the attachment of large biomolecules on the target nanoparticles [67-69]. The major advantage of the approach of nanoparticle sensing compared to the use of fluorophores is that it offers a label-free method with stable photon extinction without blinks or bleaching of the particles [66]. Given the advantages of nanoparticle-based sensing, the initial concept of colorimetric detection is demonstrated with examples such as a binding event of molecules [70, 71], the detection of the chirality of a protein [72], and the precipitation of an immunoassay-based reaction [73,74]. The representative approach for the colorimetric detection of the protein level was devised by Chen et al. [75]. In this method, nanoparticles are applied to ELISA with single-molecule sensitivity, and are functionalized by biotin and streptavidin-horseradish peroxide (HRP). Attachment onto the nanoparticles is achieved via biotin-streptavidin interaction, as shown in Figure 4(a). The spectral imaging technique serves to detect a localized precipitation reaction from the HRP enzyme, which can amplify the shift of the LSPR scattering wavelength corresponding to the change of the refractive index. In Figure 4(b), the estimated amount of attached HRP per nanoparticle at the lowest concentration is investigated to convert the single-particle peak shifts depending on the amount of HRP. From this experiment, the accurate single-molecule level detection can be determined using single gold nanostructure arrays.

To amplify the colorimetric sensing of the nanoparticles, the plasmonic coupling effect is demonstrated by forming a dimer and assembly structure between the nanoparticles [76-78]. The assemblies were created by controlling the gap distance and the satellite particle sizes. The shift of the scattering wavelength depending on the distance between the particles is calculated by [79]:

In this equation, λ is the plasmonic wavelength of the single nanoparticles, and $\Delta\lambda$ denotes the change in the plasmonic resonance wavelength of the nanoparticle when the dimer or small particles are attached. In addition, s is the gap size between the particles, and the D is the size of the single particles. Here, τ is the exponential coupling decay length of the coupled particles, and A is a pre-exponential fitting factor. Depending on the equation, the red-shift wavelength is quantitatively measured. The coupling is strongly influenced by the gap distance, as noted in the equation; hence, the individual 'plasmonic ruler' approach is shown to control the length of the gap and the type of functionalization [80,81]. There are very different peak shifts depending on the change of the gap, ranging from 2.5 nm to 0.5 nm, while a slight peak shift occurs based on the type of functionalization. Thus, the selection of the proper gap size within the visible range and the appropriate functionalization type are the important factors for the concept of plasmonic ruler. Considering these factors, Park et al. recently demonstrated the

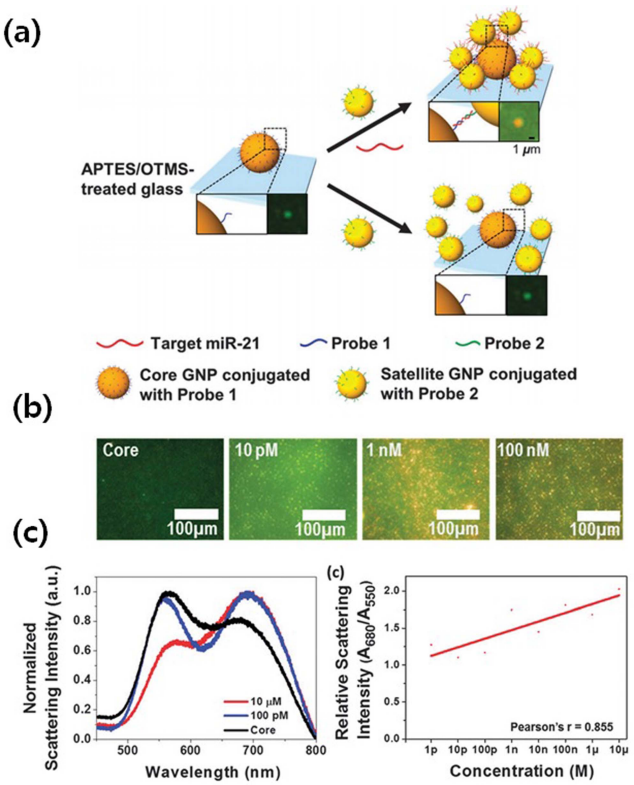

Figure 5. (a) Illustration of the formation of a core-satellite assembly on a glass substrate, (b) dark-field microscopy images corresponding to the concentration of target miRNA, and (c) changes of the spectral shift and relative intensity depending on the concentration (Parts a, b, c, and d reprinted with permission from 79 © Royal Society of Chemistry).

colorimetric detection of miRNA based on a core-satellite assembly [82]. They showed remarkable change of the scattering color and spectra at the picomolar level of biomolecules with high sensitivity, as illustrated in Figure 5. The green color of the 50-nm gold nanoparticles changes when the target molecules are attached onto the nanoparticles while linking the assemblies via specific probe molecules (Figure 5(a)). In Figure 5(b), the dark-field microscopy images show the changes of the nanoparticle color corresponding to the concentration of the miRNA with strong shift to red-scattering. In addition, the relative intensity of the scattering wavelength increases when the concentration of the miRNA increases (Figure 5 (c)). This approach represents the label-free and on-chip colorimetric detection of miRNA via targeted assemblies. This colorimetric detection method is based on a hybridizing method involving the mixing of APTES and OTMS. When optimally controlling the density of the APTES: OTMS, the core gold nanoparticles become stably attached while emitting the green color and the color shifts to red for core-satellite nano-assemblies hybridized with miRNA. This hybridization step and corresponding color change in the visible range is very important for colorimetric detection. The unique core-satellite assemblies which enhance the nanoplasmonic effect can be extended

to the lab-on-a-chip platform, especially as POCT for low-resource environments.

IV. Scalable Fabrication of Nanoplasmonic sensing Platform

With the help of nanotechnology, the highly sensitive detection of optical information and target biomolecules by nanoplasmonics is investigated with various and unique nanostructures. This sensing approach wholly depends on the nanofabrication process, whether it relies on a focused ion beam (FIB) [83,84], e-beam lithography [85, 86], or extreme ultraviolet lithography (EUV) [87] to realize top-down nanopatterning and a self-assembly layer for the attachment of nanoparticles [88] using electrostatic or van-der Waals force. However, these patterning processes have various problems. When making a pattern of a large dimension, a considerable amount of time is required to complete the process, and the cost associated with creating the purposed nanoscale pattern can be high. In addition, controlling the electron, ion, and light beam sizes uniformly in nanoscale can be quite challenging especially for large area. The target substrates also cause problems related to electron charging on an insulating substrate such as glass or polymer. Therefore, more scalable approach is desired for nanoscale patterning. Nanoscale printing techniques such as nanostencil printing [89], nanoimprint lithography [90,91], or nanosphere or colloidal lithography [92,93] as well as contact transfer printing methods [94] have been demonstrated and found to be cost-effective methods for large scale printing on unconventional substrates.

With the help of these unconventional printing techniques, the emerging nanoplasmonic devices can feasibly provide new capabilities for optical devices, integrated circuits, and sensing platforms. Nanostencil lithography, as shown in Figure 6, achieved a high throughput process, producing low-cost flexible plasmonic and metamaterials [89]. This process provides a simple and eidetic method using a stencil in the role of a mask for the patterning process. The resolution limitation of the stencil patterning is a gap size of 25 nm with sub-100 nm dimension on an unconventional substrate. Another repeatable printing method is the direct imprinting process, which can be extended to flexible devices with simple fabrication processes [95]. Researchers have also fabricated complex structures such as flowers by means of chemical modification with trans-1,2-bis(4-

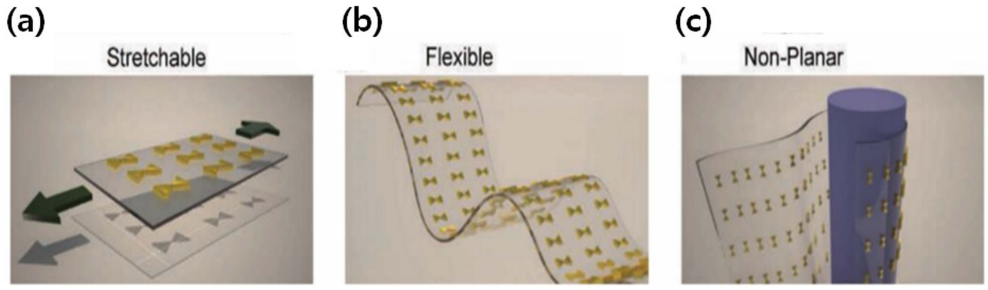

Figure 6. Flexible plasmonics on (a) stretchable, (b) flexible, and (c) non-planar substrates by means of stencil lithography (Parts a, b, and c reprinted with permission from 86, © Wiley).

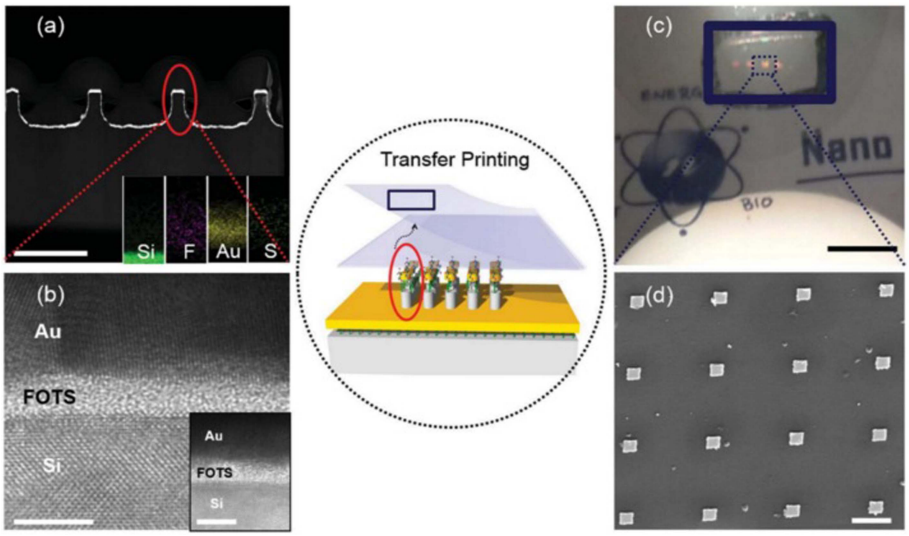

Figure 7. Contact transfer printing of flexible nanoplasmonics: (a) TEM image of a master mold functionalized by FOTS, gold, and a biofunctional group, (b) high-resolution TEM images of the master mold, (c) photographic image of the transferred nanostructures on a flexible substrate, and (d) SEM image of gold nanostructure array (Parts a, b, and c reprinted with permission from 93, © Wiley).

pyridly)ethylene (BPE) [96]. This chemical serves to connect the adjacent gold to pyridyl nitrogen to create a nanoscale gap without additional patterning. This method is a scalable fabrication scheme for the realization of various structures by combining top-down imprinting and bottom up-chemical linkage approaches. Recently, Lee et al. demonstrated a flexible nanoplasmonics sensing platform using a scalable contact transfer printing method as shown in Figure 7 [97]. Using a release layer of trichloro(1H, 1H, 2H, 2H-perfluorooctyl)silane (Figures 7(a)-(b)), stable contact transfer printing of the nanostructure is achieved on a flexible substrate. Also, biofunctionalization is included on the side-edge of the target nanostructure for the enhancement of the electric field, thus the sensing signals. The scattering color shown in the photographic image of Figure 7(c) is red from the nanoplasmonic arrays as shown in the magnified scanning microscopy image in Figure 7 (d). Careful integration of the contact transfer printing and a chemical functionalization process enabled the noise-free sensing with pre-functionalization and the side-edge enhancement of the electric field for bioapplications on a flexible platform.

Unlike traditional fabrication methods, these fabrication processes allow an adequately scalable and reliable process for the fabrication of high density arrays of nanostructures in large dimension, thus enabling next-generation plasmonic devices for flexible, wearable, and biocompatible applications.

V. Conclusions

In this review, we have discussed nanoplasmonics as an enabling platform, especially for integrated sensing capabilities among various aspects of this technology. For the applications in integrated photonic interconnection, nanoplasmonic photodetectors based on a uniquely shaped metallic nanostructure provides the size compatibility with electronics while also demonstrating high responsivity, low power operation, and the broadband detection. With the advancements in nanophotonics, the future optical interconnects will migrate into more integration with CMOS electronics requiring further compatibility in fabrication. Therefore, emeging nanoplasmonic components will need more compatible alternative materials such as conventional metal nitrides, semiconductors, transparent conducting oxides, and 2D materials [98-100].

In terms of the sensing capability for biomolecule detection, the enhancement of the sensitivity and good selectivity for the detection of protein levels and nucleotide levels is achievable using a single nanoparticle or core-satellite nanoparticle assemblies based on nanoplasmonics. A combination of microfluidics and high resolution spectroscopy from plasmonic sensing devices can push beyond the hurdles of practical bioapplications. Moreover, new chemical and biological quantification techniques, investigations of binding kinetics, molecular identifications for multiplexing diagnostics with therapy in what is known as theranostics represent remaining research areas in relation to novel biosensing applications [101-103].

Acknowledgments

This research was supported by the MSIP (Ministry of Science, ICT and Future Planning) of Korea under the “IT Consilience Creative Program” (IITP-2015-R0346-15-1008) supervised by the IITP (Institute for Information & Communications Technology Promotion).

References

[1] J. G. Webster and H. Eren, *Measurement, Instrumentation, and Sensors Handbook: Spatial, Mechanical, Thermal, and Radiation Measurement* vol. 1 (CRC press, Florida 2014), pp. I-7-I-9.
[2] J. Fraden, *Handbook of modern sensors: physics, designs, and applications* (Springer Science & Business Media, San Diego, 2004), pp. 37-119.
[3] X. Chen, Z. Guo, G.-M. Yang, J. Li, M.-Q. Li, J.-H. Liu, and X.-J. Huang, *Mater. Today,* 13, 28 (2010).
[4] J. Wang, *Analyst,* 130, 421 (2005).
[5] I. Obataya, C. Nakamura, S. Han, N. Nakamura, and J. Miyake, Biosens. Bioelectron, 20, 1652 (2005).
[6] P. F. Davies, J. Vasc. Surg. 13, 729 (1991).
[7] C. J. Murphy, Anal. Chem. 74, 520A (2002).
[8] J. M. López-Higuera, *Handbook of optical fibre sensing technology* (John Wiley & Sons, Chichester, 2002)
[9] A. Yalcin, K. C. Popat, J. C. Aldridge, T. Desai, J. Hryniewicz, N. Chbouki, *B. E. Little, O. King, V. Van, C. Sai, D. Gill, M. Anthes-Washburn, M. S. Unlu, and B. B. Goldberg, IEEE J. Sel. Top. Quantum Electron.* 12, 148 (2006).
[10] L. E. Kreno, K. Leong, O. K. Farha, M. Allendorf, R. P. Van Duyne, and J. T. Hupp, *Chem. Rev.* 112, 1105 (2011).
[11] S. C. Rashleigh, *Opt. Lett.* 5, 392 (1980).
[12] H. Kaplan, *Practical applications of infrared thermal sensing and imaging equipment* vol. 75 (SPIE press,Washington, 2007) pp. 9-29.
[13] M. R. Leahy-Hoppa, J. Miragliotta, R. Osiander, J. Burnett, Y. Dikmelik, C. McEnnis, and *J. B. Spicer, Sensors,* 10, 4342-4372 (2010).
[14] P. Han and X.-C. Zhang, Appl. Phys. Lett. 73, 3049 (1998).
[15] B. MacCraith, V. Ruddy, C. Potter, B. O’Kelly, and J. McGilp, *Electron. Lett.* 27, 1247 (1991).
[16] R. Yotter and D. M. Wilson, *IEEE Sens. J.* 3, 288 (2003).
[17] O. M. Maragò, P. H. Jones, P. G. Gucciardi, G. Volpe, and A. C. Ferrari, *Nat. Nanotechnol.* 8, 807 (2013).
[18] S. A. Maier, *Plasmonics: fundamentals and applications* (Springer Science & Business Media, New York, 2007), pp. 65-80.
[19] H. A. Atwater, *Sci. Am.* 296, 56 (2007).
[20] H. Duan, A. I. Fernández-Domínguez, M. Bosman, S. A. Maier, and J. K. Yang, *Nano lett.* 12, 1683 (2012).
[21] M. I. Stockman, *Phys. Today,* 64, 39 (2011).
[22] G. Baffou and R. Quidant, *Chem. Soc. Rev.* 43, 3898 (2014).
[23] A. Dmitriev, *Nanoplasmonic sensors* (Springer Science & Business Media, New York, 2012) pp. 105-126.
[24] Y. Shen, J. Zhou, T. Liu, Y. Tao, R. Jiang, M. Liu, *G. Xiao, J. Zhu, Z. -K. Zhou, X. Wang, C. Jin, and J. Wang, Nat. Commun.* 4, 2381 (2013).
[25] A. Kabashin, P. Evans, S. Pastkovsky, W. Hendren, G. Wurtz, R. Atkinson, *R. Pollard, V. A. Podolskiy, and A. V. Zayats, Nat. Mater.* 8, 867 (2009).
[26] T. Chung, S.-Y. Lee, E. Y. Song, H. Chun, and B. Lee, *Sensors,* 11, 10907 (2011).
[27] H. Liao, C. L. Nehl, and J. H. Hafner, Nanomedicine, 1, 201 (2006).
[28] A. J. Gormley, N. Larson, S. Sadekar, R. Robinson, A. Ray, and H. Ghandehari, *Nano today,* 7, 158 (2012).

[29] J. R. Cole, N. A. Mirin, M. W. Knight, G. P. Goodrich, and N. J. Halas, *J. Phys. Chem. C,* 113, 12090 (2009).
[30] A. Alu and N. Engheta, *J. Opt. A-Pure. Appl. Op.* 10, 093002 (2008).
[31] Y. Cui, R. S. Hegde, I. Y. Phang, H. K. Lee, and X. Y. Ling, *Nanoscale,* 6, 282 (2014).
[32] A. Fatima, I. Mehra, and N. K. Nishchal, Proceedings of the 2014 *International Conference on Fibre Optics and Photonics*, (Kharagpur India, 13-16 December 2014) p. S5A. 52.
[33] R. Zia, J. A. Schuller, A. Chandran, and M. L. Brongersma, *Mater. Today,* 9, 20 (2006).
[34] M. L. Brongersma, R. Zia, and J. Schuller, *Appl. Phys. A,* 89, 221 (2007).
[35] V. K. Valev, A. V. Silhanek, B. De Clercq, W. Gillijns, Y. Jeyaram, X. Zheng, *V. Volskiy, O. A. Aktsipetrov, G. A. E. Vandenbosch, M. Ameloot, V. V. Moshchalkov, and T. Verviest*, *small,* 7, 2573 (2011).
[36] S. A. Maier, Nature Photon. 2, 460 (2008).
[37] J. Dionne, H. Lezec, and H. A. Atwater, *Nano lett.* 6, 1928 (2006).
[38] P. Bai, M.-X. Gu, X.-C. Wei, and E.-P. Li, *Opt. Express,* 17, 24349, (2009).
[39] Y. Yang, Q. Li, and M. Qiu, *Scientific reports,* 6, 19490 (2016).
[40] E. Ozbay, *science,* 311, 189 (2006).
[41] A. Alu and N. Engheta, Nature Photon. 2, 307 (2008).
[42] D. P. Fromm, A. Sundaramurthy, P. J. Schuck, G. Kino, and W. Moerner, *Nano lett.* 4, 957 (2004).
[43] E. Cubukcu, E. A. Kort, K. B. Crozier, and F. Capasso, *Appl. Phys. Lett.,* 89, 093120 (2006).
[44] P. Neutens, P. Van Dorpe, I. De Vlaminck, L. Lagae, and G. Borghs, Nature Photon. 3, 283 (2009).
[45] A. Crut, P. Maioli, N. Del Fatti, and F. Vallée, *Chem. Soc. Rev.* 43, 3921 (2014).
[46] J. H. Son, B. Cho, S. Hong, S. H. Lee, O. Hoxha, A. J. Haack, *and L. P. Lee*, *Light. Sci. Appl.* 4, e280 (2015).
[47] A. Glass, P. F. Liao, D. Olson, and L. Humphrey, Opt. Lett. 7, 575 (1982).
[48] A. Sellai, *Nucl. Instr. Meth. Phys. Res. A.* 504, 170 (2003).
[49] M. Rahman, A. Karakashian, S. Broude, and D. Gladden, *Appl. Opt.* 30, 2935 (1991).
[50] J. Hetterich, G. Bastian, N. Gippius, S. Tikhodeev, G. Von Plessen, and U. Lemmer, *IEEE J. Quant. Electron.* 43, 855 (2007).
[51] T. Ishi, J. Fujikata, K. Makita, T. Baba, and K. Ohashi, *Jpn. J. Appl. Phys.* 44, L364 (2005).
[52] P. Berini, *Laser Photon. Rev.* 8, 197 (2014).
[53] J.-H. Kim and J.-S. Yeo, *Nano lett.* 15, 2291 (2015).
[54] J. Miao, W. Hu, Y. Jing, W. Luo, L. Liao, A. Pan, *S. Wu, J. Cheng, X. Chen, and W. Lu, Small,* 11, 2392 (2015).
[55] B. Radisavljevic, A. Radenovic, J. Brivio, V. Giacometti, and A. Kis, *Nat. Nanotechnol.* 6, 147 (2011).
[56] Z. Yin, H. Li, H. Li, L. Jiang, Y. Shi, Y. Sun, *G. Lu, Q. Zhang, X. Chen, and H. Zhang, ACS Nano,* 6, 74 (2011).
[57] A. Ashimoto, C. Chen, I. Bakker, and J. Slots, "Polymerase chain reaction detection of 8 putative periodontal pathogens in subgingival plaque of gingivitis and advanced periodontitis lesions," *Oral. Microbiol. Immun.* 11, 266 (1996).
[58] P. Grauballe, B. Vestergaard, A. Meyling, and J. Genner, *J. Med. Virol.* 7, 29 (1981).
[59] D. Muir, S. Varon, and M. Manthorpe, *Anal. Biochem.* 185, 377 (1990).
[60] F. Girosi, S. S. Olmsted, E. Keeler, D. C. H. Burgess, Y.-W. Lim, J. E. Aledort, *M. E. Rafael, K. A. Ricci, R. Boer, L. Hilborne, K. P. Derose, M. V. Shea, C. M. Beighley, C. A. Dahl, and J. Wasserman, Nature,* 444, 3 (2006).
[61] T. S. Hauck, S. Giri, Y. Gao, and W. C. Chan, Adv. Drug Deliv. Rev. 62, 438 (2010).
[62] X. Huang, P. K. Jain, I. H. El-Sayed, and M. A. El-Sayed, Nanomedicine, 2, 681 (2007).
[63] S. Kumar, N. Harrison, R. Richards-Kortum, and K. Sokolov, *Nano lett.* 7, 1338 (2007).
[64] O. Limaj, D. Etezadi, N. J. Wittenberg, D. Rodrigo, D. Yoo, S.-H. Oh, Hatice altug, *Nano letters,* 2016. DOI: 10.1021/acs.nanolett.5 b05316
[65] K.-L. Lee, M.-L. You, C.-H. Tsai, E.-H. Lin, S.-Y. Hsieh, M.-H. Ho, J. -C. Hsu, and P. -K. Wei, *Biosensors and Bioelectronics,* 75, 88 (2016).
[66] J. N. Anker, W. P. Hall, O. Lyandres, N. C. Shah, J. Zhao, and R. P. Van Duyne, *Nat. Mater.* 7, 442 (2008).
[67] V. Myroshnychenko, J. Rodríguez-Fernández, I. Pastoriza-Santos, A. M. Funston, C. Novo, P. Mulvaney, *L. M. Liz-Marzan, and F. J. G. de Abajo, Chem. Soc. Rev.* 37, 1792 (2008).
[68] M. A. Otte, B. Sepulveda, W. Ni, J. P. Juste, L. M. Liz-Marzán, and L. M. Lechuga, *ACS Nano,* 4, 349 (2009).
[69] B. Sepúlveda, P. C. Angelomé, L. M. Lechuga, and L. M. Liz-Marzán, *Nano Today,* 4, 244 (2009).
[70] M. E. Stewart, C. R. Anderton, L. B. Thompson, J. Maria, S. K. Gray, J. A. Rogers, *and R. G. Nuzzo, Chem. Rev.* 108, 494 (2008).
[71] I. Choi and Y. Choi, *IEEE J. Sel. Top. Quantum Electron.* 18, 1110 (2012).
[72] J. R. L. Guerreiro, M. Frederiksen, V. E. Bochenkov, V. De Freitas, M. G. Ferreira Sales, and D. S. Sutherland, *ACS Nano,* 8, 7958 (2014).
[73] S. Lee, K. M. Mayer, and J. H. Hafner, *Anal. chem.* 81, 4450 (2009).
[74] K. M. Mayer, S. Lee, H. Liao, B. C. Rostro, A. Fuentes, P. T. Scully, *C. L. Nehl, and J. H. Hafner, ACS Nano,* 2, 687 (2008).
[75] S. Chen, M. Svedendahl, R. P. V. Duyne, and M. Kall, *Nano lett.* 11, 1826 (2011).
[76] P. K. Jain and M. A. El-Sayed, *Chem. Phys. Lett.* 487, 153 (2010).
[77] C.-Y. Tsai, J.-W. Lin, C.-Y. Wu, P.-T. Lin, T.-W. Lu, and P.-T. Lee, *Nano lett.* 12, 1648 (2012).
[78] X. Qian, X. Zhou, and S. Nie, *J. Am. Chem. Soc.* 130, 14934 (2008).
[79] C. Tabor, D. Van Haute, and M. A. El-Sayed, *ACS Nano,* 3, 3670 (2009).
[80] J. H. Yoon and S. Yoon, *Langmuir,* 29, 14772 (2013).
[81] P. K. Jain, X. Huang, I. H. El-Sayed, and M. A. El-Sayed, *Plasmonics,* 2, 107 (2007).
[82] J. Park and J.-S. Yeo, *Chem. Commun.* 50, 1366, (2014).
[83] A. A. Tseng, *Small,* 1, 924 (2005).
[84] S. Matsui, T. Kaito, J.-i. Fujita, M. Komuro, K. Kanda, and Y. Haruyama, *J. Vac. Sci. Technol. B,* 18, 3181 (2000).
[85] C. Vieu, F. Carcenac, A. Pepin, Y. Chen, M. Mejias, A. Lebib, *L. Mannin-Ferlazzo, L. Couraud, and H. Launois, Appl. Surf. Sci.* 164, 111 (2000).
[86] H. Seyringer, B. Fünfstück, and F. Schäffler, The Society of Microelectronics-Annual Report 1999
[87] B. Wu and A. Kumar, *J. Vac. Sci. Technol. B,* 25, 1743 (2007).
[88] Q. Li, J. Zheng, and Z. Liu, *Langmuir,* 19, 166 (2003).
[89] S. Aksu, M. Huang, A. Artar, A. A. Yanik, S. Selvarasah, M. R. Dokmeci, *and H. Altug, Adv. Mater.* 23, 4422 (2011).
[90] S.-W. Lee, K.-S. Lee, J. Ahn, J.-J. Lee, M.-G. Kim, and Y.-B. Shin, *ACS Nano,* 5, 897 (2011).
[91] J. A. Rogers and R. G. Nuzzo, *Mater. Today,* 8, 50 (2005).
[92] C. L. Haynes and R. P. Van Duyne, *J. Phys. Chem. B,* 105, 5599 (2001).
[93] H. Fredriksson, Y. Alaverdyan, A. Dmitriev, C. Langhammer, D. S. Sutherland, M. Zäch, *and B. Kasemo*, *Adv. Mater.* 19, 4297 (2007).
[94] Z. Fan, J. C. Ho, Z. A. Jacobson, R. Yerushalmi, R. L. Alley, H. Razavi, *and A. Javey, Nano lett.* 8, 20 (2008).
[95] D. Y. Khang, H. Yoon, and H. H. Lee, *Adv. Mater.* 13, 749 (2001).
[96] S. J. Barcelo, A. Kim, W. Wu, and Z. Li, *ACS Nano,* 6, 6446 (2012).
[97] J. Lee, J. Park, J. Y. Lee, and J. S. Yeo, *Adv. Sci.* 2, 1500121, (2015).
[98] G. V. Naik, V. M. Shalaev, and A. Boltasseva, *Adv. Mater.* 25, 3264 (2013).
[99] N. Kinsey, M. Ferrera, V. Shalaev, and A. Boltasseva, *J. Opt. Soc. Am.* 32, 121 (2015).
[100] Y. Zhong, S. D. Malagari, T. Hamilton, and D. Wasserman, *J. Nanophotonics,* 9, 093791 (2015).
[101] J. C. Ndukaife, A. Mishra, U. Guler, A. G. A. Nnanna, S. T. Wereley, and A. Boltasseva, *ACS Nano,* 8, 9035 (2014).
[102] P. Chen, M. T. Chung, W. McHugh, R. Nidetz, Y. Li, J. Fu, *T. T. Cornell, T. P. Shanley, and K. Kurabayashi, ACS Nano,* 9, 4173 (2015).
[103] X. Wang, Y. Cui, and J. Irudayaraj, *ACS Nano, 9, 11924 (*2015).